Sergei N. Magonov, Myung-Hwan Whangbo

Surface Analysis with STM and AFM

Experimental and Theoretical Aspects of Image Analysis

Weinheim · New York · Basel · Cambridge · Tokyo

Sergei N. Magonov, Myung-Hwan Whangbo

Surface Analysis with STM and AFM

Also of Interest

- E. Lifshin (ed.) **Characterization of Materials**
  Volumes 2A and 2B from the series *Materials Science and Technology,* edited by R. W. Cahn, P. Haasen, E. J. Kramer
  Volume 2A, VCH 1992. Volume 2B, VCH 1994.

- N. J. DiNardo **Nanoscale Characterization of Surfaces and Interfaces,** VCH 1994.

- S. Amelinckx, D. Van Dyck, J. F. Van Landuyt, G. Van Tendeloo (eds.) **Handbook of Microscopy.** Volume 1. **Methods.** Volume 2. **Applications in Materials Science,** VCH 1996.

- D. A. Bonnell **Scanning Tunneling Microscopy and Spectroscopy. Theory, Techniques and Applications,** VCH 1995.

- K. Wetzig, D. Schulze **In Situ Scanning Electron Microscopy in Materials Research,** Akademie Verlag 1995.

Distribution:
VCH, P.O. Box 101161, D-69451 Weinheim (Federal Republic of Germany)
Switzerland: VCH P.O. Box, CH-4020 Basel (Switzerland)
United Kingdom and Ireland: VCH (UK) Ltd., 8 Wellington Court, Cambridge CB1 1HZ (England)
USA and Canada: VCH, 220 East 23rd Street, New York, NY 10010-4606 (USA)
Japan: VCH, Eikow Building, 10-9 Hongo 1-chome, Bunkyo-ku, Tokyo 113 (Japan)

ISBN 3-527-29313-2

Sergei N. Magonov, Myung-Hwan Whangbo

Surface Analysis with STM and AFM

Experimental and Theoretical Aspects of Image Analysis

Weinheim · New York · Basel · Cambridge · Tokyo

Dr. S. N. Magonov
Digital Instruments
520 E. Montecito St.
Santa Barbara, CA 93103
USA

Dr. M.-H. Whangbo
Department of Chemistry
North Carolina State Univ.
Raleigh, NC 27695-8204
USA

Published jointly by
VCH Verlagsgesellschaft mbH, Weinheim (Federal Republic of Germany)
VCH Publishers, Inc., New York, NY (USA)

Editorial Directors: Dr. Peter Gregory, Dr. Ute Anton
Production Manager: Dipl.-Wirt.-Ing. (FH) Bernd Riedel

Library of Congress Card No. applied for.

A catalogue record for this book is available from the British Library.

Die Deutsche Bibliothek Cataloguing-in-Publication Data:

Magonov, Sergei N.:
Surface analysis with STM and AFM : experimental and
theoretical aspects of image analysis / Sergei N. Magonov ;
Myung-Hwan Whangbo. – Weinheim ; New York ; Basel ;
Cambridge ; Tokyo : VCH, 1996
ISBN 3-527-29313-2
NE: Whangbo, Myung-Hwan:

Composition: Filmsatz Unger & Sommer GmbH, D-69469 Weinheim
Printing: Strauss Offsetdruck GmbH, D-69509 Mörlenbach
Bookbinding: Wilh. Osswald & Co., D-67433 Neustadt

Printed in the Federal Republic of Germany

Preface

Scanning tunneling microscopy (STM) and atomic force microscopy (AFM) are powerful tools for the examination of surfaces. The research, development, and application of the STM and AFM methods are currently making rapid progress. As a result, a large number of papers are being published every year on diverse subjects, from theory to experiment as well as on applications to a variety of materials. This makes it rather difficult for an individual to keep up with such fast development. The physical concepts employed in the instrumentation of STM and AFM are simple, but the interpretation of the STM and AFM results can be complicated because of the convolution of several interactions in the measurement process. This complication exists in the large-scale imaging of surface morphology as well as in the molecular- and atomic-scale images. Thus, many STM and AFM studies can be misinterpreted. To help to alleviate this problem, we felt it necessary to bring together into a book the essential components of STM and AFM studies, namely the practical aspects of STM and AFM, the image simulation by surface electron density plot calculations, and the qualitative evaluation of tip force induced surface corrugations.

The primary goal of this book is to describe how the surfaces of various materials are characterized by employing STM and AFM, and what physical/chemical features can be deduced from their images. The text consists of three parts. The first part is concerned with the backgrounds and fundamentals of STM and AFM, the physical phenomena leading to these methods, and the practical aspects of imaging. The second part describes the theoretical aspects of image analysis, the density plot calculations, and the accommodation of tip–sample force interactions. The third part deals with the experimental STM and AFM images and their interpretation for a variety of materials, which include layered inorganic materials, organic conducting salts, organic adsorbates at solid/liquid interfaces, self-assembled amphiphiles, and polymers. The experimental examples described here have mostly been taken from our own original publications.

This book is designed to be a reference work for researchers already involved in STM and AFM as well as for newcomers to the field. It can also be used as a text for a one-semester special-topic course on STM/AFM applications at the graduate level.

The authors would like to thank their colleagues Dr. Georg Bar, Hardy Bengel, Konrad Crämer, Alexander Wawkuschewski, Dr. Igor Tuzov, Dr. Jingqing Ren, Dr. Weigen Liang, Jeffrey Paradis, Professor Dongwoon Jung, and Dong-Kyun Seo. The writing of this book would not have been possible without their experimental

and theoretical studies. Professor H.-J. Cantow is specially thanked for his continuous support for and interest in our work. The authors also thank Professor R. Brec, Dr. M. Evain, Professor G. Koßmehl, Professor M. Möller, Professor R. Mülhaupt, Professor J. Peterman, Dr. B. Pfannemüller, Professor M. Schwörer, Professor G. Thiele and Professor E. Yagubskii for making their samples available to us. Dr. V. Elings, Professor P. Hansma and Professor B. Parkinson are acknowledged for invaluable discussions concerning various aspects of STM and AFM. Hardy Bengel and Konrad Crämer are thanked for their help in preparing the figures and diagrams used in this book. M.-H. W. thanks the Alexander von Humboldt Foundation for a Humboldt Research Award for Senior US Scientists, which made possible his extended visit to the Materials Research Center, Albert-Ludwigs University, where the writing was completed. Finally, the authors thank their wives, Elena and Jin-Ok, and their children, Katja, Masha, Jennifer, and Albert, for their patience and moral support.

Our joint research activities have been supported by the US Department of Energy, Office of Basic Sciences, Division of Materials Sciences, under Grant DE-FG05-86ER45259, and by the European Community under the Human Capital and Mobility Project (ERBCHRXCT940675).

Freiburg, Germany
Raleigh, North Carolina, USA
November 1995

Sergei N. Magonov
Myung-Hwan Whangbo

Contents

1 Introduction

1.1 Development of Scanning Probe Microscopy

The invention of a scanning tunneling microscope nicely exemplifies the creation of a new research tool by innovative implementation of scientific and technological knowledge, thereby further advancing fundamental science and technology. The quantum-mechanical phenomenon of electron tunneling had been known for a long time, but the use of this phenomenon for the imaging of a conducting surface on atomic scale was realized only in 1982 when the first scanning tunneling microscope was built by Binnig et al [1]. At present, scanning tunneling microscopy (STM) is a powerful tool for analyzing metallic and semiconducting surfaces. The most important feature of STM is the real-space visualization of surfaces on atomic scale. What is converted into an image in STM is either the spatial variation of the tunneling current or the spatial variation of the tip height. The tunneling current decreases exponentially with increasing tip–sample distance. Thus, at any given location of the tip over the sample surface, the electron transfer involves only one atom, or only a few atoms, at the tip apex and on the surface closest to them. This gives rise to the local character of STM measurements, which makes it possible to visualize surface structures with sub-angstrom resolution and to detect various atomic-scale defects that are inaccessible by diffraction and spectroscopic techniques [2–4]. In addition, STM is used to examine adsorbate structures and dynamic phenomena on surfaces (e.g., diffusion and chemical reactions).

Since a tunneling current is employed in STM, the application of this method is mostly limited to metals and semiconductors. To enable the detection of atomic-scale features of insulating surfaces, an atomic force microscope was invented [5]. In atomic force microscopy (AFM) it is commonly the repulsive force between the tip (located at the end of a cantilever) and sample that is measured, on the basis of the cantilever deflection. In this contact-mode AFM, the spatial variation of the tip–sample repulsive force or that of the tip height is converted into an image. Because the repulsive force is universal, AFM is applicable to conducting as well as insulating materials. In general, AFM enables one to detect surface morphology, nanoscale structures, and molecular- and atomic-scale lattices.

Contact-mode AFM was originally introduced for high-resolution surface profiling. With the progress in AFM applications, it became clear that for many materials this objective can be achieved only by minimizing tip–sample force interactions, because the latter may modify the topography of a sample surface. In addition, it was also realized that these interactions can be utilized to probe the mechanical properties of surfaces such as indentation, adhesion and friction. For example, the tip may cause

elastic or inelastic surface deformations [6], which can be recognized from the images obtained with high forces. In imaging with low force, the influence of the weak surface forces (e.g., van der Waals, hydrophilic, hydrophobic, and electrostatic interactions) on the cantilever movement becomes significant [7]. It is a challenging task to deconvolute the contributions of these forces to the image contrast. Invaluable information about the tip-sample force interactions can be obtained by analyzing the force versus tip-sample distance curves (hereinafter referred to as force-vs.-distance curves).

The success of STM and AFM led to a new family of scanning probe techniques in which different types of tip-sample interactions are utilized. For further details of these methods, the reader is referred to several reviews and books [2-4]. So far, STM and AFM are the most advanced scanning probe methods and the only ones providing atomic-resolution images. AFM has found much broader application than STM and is currently the dominant scanning probe technique.

1.2 Key Problems of STM and AFM Applications

The development of instrumentation and the availability of commercial microscopes at moderate price have accelerated the use of STM and AFM and demonstrated their unique potential in surface characterization. In applying STM and AFM to surfaces of chemical interest, common problems to be faced are how to distinguish genuine features from experimental artifacts in observed images, how to improve the image resolution, how to collect comprehensive experimental information, and how to interpret observed images (especially those with atomic or molecular resolution). A close interplay between experiment and theory is essential in answering these questions and in making STM and AFM truly indispensable analytical tools for surface science and nanotechnology.

1.2.1 Image Interpretation

Atomic-scale STM and AFM images are routinely recorded for many crystalline surfaces, but their interpretation is by no means straightforward. It is tempting to assign the atomic-size spots of STM and AFM images to the surface atomic or molecular structures. Such a correspondence has been found in several cases, but this interpretation can be misleading, especially for STM, because the electron tunneling involves only the energy levels of the sample lying in the vicinity of the Fermi level e_f. When the tip-sample interactions are neglected, the STM image is described by the partial electron density plot $\rho(r_0, e_f)$ of the sample surface [8]. In contact-mode AFM measurements, all the electrons of the surface atoms are involved in the repulsive interac-

tions with the tip, so that the AFM image is described by the total electron density plot $\rho(r_0)$ of the surface. Consequently, it is reasonable to assign the AFM images to the surface topography, but this is not necessarily the case in STM.

When the geometry of a sample is known, it is straightforward to calculate the $\rho(r_0, e_f)$ plots from its electronic structure. For a layered material, the surface reconstruction is negligible so that the geometry of the surface layer is well approximated by the layer geometry of the bulk crystal structure. For a large number of organic and inorganic layered materials, the atomic- and molecular-scale features of their STM images [9] have been successfully interpreted on the basis of the $\rho(r_0, e_f)$ plots calculated with the extended Hückel tight binding (EHTB) electronic band structure method [10].

In general, the contribution of an atom to the $\rho(r_0, e_f)$ plot increases as its distance to the tip decreases and as its electronic contribution to the energy levels around the Fermi level increases. Since the more-protruding atoms do not necessarily make more contributions to the energy levels near the Fermi level, it is difficult to interpret STM images unless appropriate partial density plots are calculated, even when the geometry of the sample surface is known. The essential findings of the STM studies carried out in conjunction with $\rho(r_0, e_f)$ plot calculations [9] can be summarized as follows:

(a) When the height corrugation of the surface is of the order of 0.5 Å, the lower-lying atoms of the surface can dominate the $\rho(r_0, e_f)$ plot and hence the STM image.
(b) If the subsurface atoms lie more than 1 Å (0.1 nm) below the surface atoms, the STM patterns are dominated by the topmost surface atoms, even when the energy levels around the Fermi level are dominated by the subsurface atoms.
(c) Insulating molecules adsorbed on a metallic substrate are detected by STM, because their orbitals mix slightly into the Fermi level of the metallic substrate and because they are close to the tip.

It is challenging to characterize surface reconstruction on the basis of high-resolution STM and AFM images. For this purpose, it is necessary to calculate the $\rho(r_0, e_f)$ and $\rho(r_0)$ plots for a number of model structures until a good match is found between theory and experiment.

To help interpret the STM images of semiconducting materials on the basis of partial density plot calculations, it is desirable to carry out imaging with bias voltages of different magnitudes and polarities (i.e., positive or negative). Such measurements, as well as the recording of current-vs.-voltage curves, are the subject of scanning tunneling spectroscopy (STS), which was critically reviewed by Trompt [11].

1.2.2 Tip-Sample Interactions

To be precise, the image interpretation described above is valid when the tip is point-like and the tip-sample interactions are negligible. In practice, these conditions are hardly realized. The tip-shape anisotropy can induce various artifacts in large- and atomic-scale images. Even the use of tips with perfect shape might lead to a nontrivial image perturbation because of the inevitable tip-sample interactions in STM and AFM (especially in ambient-condition experiments). The scanning tip can exert strong vertical and lateral forces on the sample, thereby causing surface deformation and removal of weakly bound and defective layers.

Consideration of the tip-sample force interactions is critical in the imaging of soft organic materials. AFM possesses a unique potential for the characterization of these materials, as has been demonstrated in studies of the self-assembled structures of saccharide-based amphiphiles [12]. On the basis of the AFM images of their adsorbates on mica, it was possible to determine the molecular packing in the bilayers, detect a variety of micellar nanostructures (disks, grains, cylinders, etc.) and characterize the topography of the supramolecular assemblies. In general, the imaging of organic compounds requires minimization of the applied force to avoid surface damage and reduce the tip-sample contact area. In contact-mode AFM the applied force is significantly diminished when the tip and sample are both immersed in liquids (e.g., water, ethanol) [7a]. To lessen the surface modification induced by the lateral force of the tip, one may employ dynamic modes (e.g., tapping-mode AFM) in which the cantilever vibrates for the tip to make an intermittent contact with the sample [13]. In the AFM of polymers, minimization of the tip-sample force interactions makes it possible to image mechanically weak surface nanostructures that are inaccessible by electron microscopy (e.g., 2-3 nm-wide nanofibrils of stretched polyethylene tapes under an applied force of ca. 2 nN [14]).

The resolution of contact-mode AFM strongly depends on the sample. On poorly ordered surfaces, the resolution is limited by the tip-sample contact area. For example, the detection of the polyethylene nanofibrils mentioned above suggests a tip-sample contact diameter smaller than 2 nm, which is consistent with the theoretical estimate [15a]. In contact-mode AFM studies of crystalline surfaces, atomic- and molecular-scale lattices are routinely observed in images obtained with different applied forces. This indicates that the image resolution for crystalline surfaces does not critically depend on the size of the contact area. In contrast to the case of STM, atomic-size defects are hardly detected in AFM images.

Strong tip-sample force interactions are common for ambient-condition STM measurements. In air, a sample surface is coated with a liquid contamination layer (mostly made up of water). Therefore, while scanning the surface, the STM tip is in contact with the contamination layer and exerts a load (i.e., force) on the surface via this layer. This load, which is in the order of several hundreds of nanonewtons, is much higher than the typical operating force in contact-mode AFM [16]. Conse-

quently, the STM images recorded at ambient condition are more likely to represent "distorted surfaces" under the action of the tip force rather than the "ideal surfaces" one expects in the absence of the tip-sample interactions. To understand the influence of such force interactions on STM images, it is necessary to perform measurements as a function of the tip-sample separation. Typically, the force interactions become stronger with decreasing tip-sample distance. In terms of the operational parameters of STM experiments, the tip-sample distance is reduced by decreasing $R_{gap} = |V_{bias}|/I_{set}$, where V_{bias} is the bias voltage and I_{set} is the set-point tunneling current. Therefore, by conducting STM measurements at different levels of tip-sample interactions, one can also learn about the surface mechanical properties.

1.2.3 Surface Relaxation and Local Hardness

In general, the surface of a material consists of atoms with different local environments. The local area of a surface atom (i.e., the atom and its closest neighbors) can have a different hardness, depending on its local structural and chemical bonding environment. It is expected that under the tip force a harder surface region (or atom) is depressed less, and hence appears more elevated in the image, than a softer region (or atom). One can investigate the spatial variation of the local hardness in a given sample surface by analyzing depression pattern induced by the tip force, on the basis of STM or AFM measurements under several different levels of force interactions. Macroscopic deformations of materials are discussed in terms of hardness and stiffness. The hardness is defined as the load (i.e., applied force) divided by the contact area, and the stiffness as the slope of the load-vs.-depression curve [15b]. As will be discussed below, the surface local hardness (or stiffness) is a nanoscale analog of the corresponding macroscopic properties.

AFM is indispensable for the detection of surface relaxation on the nanometer and subnanometer scales. On the images of stretched polyethylene tapes, the force-dependent contrast variations reveal the presence of hard and soft nanoscale regions within a nanofibril core [14a]. The tip force might also cause conformational changes in biological macromolecules [17]. In the AFM studies of layered transition-metal tellurides MA_xTe_2 (M = Nb, Ta; A = Si, Ge), strong applied forces of up to several hundred nanonewtons induce reversible contrast changes in their atomic-scale images. In a number of layered materials (e.g., graphite, transition-metal halides) the interlayer arrangement can cause a specific hardness pattern in the topmost layer, which appears as a moiré pattern in the AFM and STM images [18]. All these observations are explained in terms of the local hardness concept. The tip-sample interactions leading to a macroscopic deformation of the tip and sample (in the region of their contact surface) have been described by the continuum theory, which neglects the presence of discrete atoms and molecules in the interacting macroscopic bodies.

The microscopic surface deformation described by the local hardness concept is not covered by the continuum theory. It is a challenging problem to bring the prediction of local hardness to a quantitative level.

What the $\rho(r_0, e_f)$ and $\rho(r_0)$ plots simulate are ideal STM and AFM images expected for a defect-free surface in the absence of tip–sample interactions. Therefore, for certain compounds, it may be inadequate to interpret the STM images in terms of electron density plots calculated for non-relaxed surface structures. In principle, a comprehensive analysis requires knowledge of the surface deformation and the associated change in the $\rho(r_0, e_f)$ plot. To estimate a possible surface reconstruction, a systematic study of AFM images with different applied forces can be useful. AFM contrast variations might indicate a local hardness variation of the surface, from which one can make a reasonable guess of the deformed surface structure needed for the electron density plot calculations. At tip forces of several hundreds of nanonewtons, the surface deformations will be similar to those expected in STM. Such an interplay between theory and experiment would be invaluable for self-consistent STM and AFM image interpretations.

1.2.4 Surface Forces and AFM

A rational examination of the tip–sample interactions in low-force imaging requires consideration of the surface forces. Tip–sample adhesion, which leads to hysteresis in the force-vs.-distance curve, is a direct consequence of the surface forces. In ambient-condition experiments this hysteresis is enhanced by the capillary forces associated with the contamination layer. In subliquid measurements, in which the capillary forces are absent, the magnitude of the hysteresis can be assigned to the tip–sample adhesion. To determine the spatial variation of the tip–sample adhesion, one may measure the force-vs.-distance curves at a large number of sample surface locations [7c, d]. Alternatively, one may determine the variation of the lateral force (rather than the vertical force employed in the force-vs.-distance curve measurements), assuming that the lateral force increases with the tip–sample adhesion [7e]. It is appealing to correlate the adhesion and lateral force variations with the chemical nature of particular surface regions. However, the relationship between the chemical nature of a surface, its morphology, and the adhesion is not well understood. Recently, hydrophilic and hydrophobic forces have attracted considerable attention. Systematic studies aimed at understanding the effects of these forces on AFM imaging are currently under active scrutiny [19]. These efforts can be facilitated by operating AFM with chemically modified probes and in different environments so as to alter deliberately the strengths of the specific surface forces. Such an approach can help, for example, to identify nanoscale surface regions with different hydrophilic and hydrophobic properties.

1.3 Objectives

This book is primarily concerned with how the surfaces of various materials are characterized by employing STM and AFM, and what physical/chemical features can be deduced from their images. To achieve these objectives, two important steps in the application of STM and AFM should be considered. One is the recording of experimental images as a function of tunneling parameters and applied forces to extract information about the surface morphology, nanostructure, and atomic-scale features. The other is the interpretation of the observed images in terms of the topographic, electronic, and mechanical properties of the surfaces.

Several monographs concerning scanning probe studies have already appeared [2–4], but their overlap with this book is minimal. Most of the examples given in this book were taken from the experimental and theoretical studies carried out by the research groups at Freiburg and Raleigh. It is hoped that the experimental and theoretical aspects of STM and AFM studies presented in this book are practical and interesting for researchers already involved in STM and AFM, as well as for newcomers to the field.

References

[1] G. Binnig, H. Rohrer, Ch. Gerber, E. Weibel, *Phys. Rev. Lett.* **1982**, *49*, 57.
[2] R. Wiesendanger, H.-J. Güntherodt (Eds.), *Scanning Tunneling Microscopy I, II* and *III*, Springer, Heidelberg, **1992** and **1993**.
[3] C. J. Chen, *Introduction to Scanning Tunneling Microscopy*, Princeton University Press, Princeton, **1993**.
[4] D. A. Bonnell (Ed.), *Scanning Tunneling Microscopy and Spectroscopy*, VCH, New York, **1993**.
[5] G. Binnig, C. Quate, Ch. Gerber, *Phys. Rev. Lett.* **1986**, *56*, 930.
[6] (a) M. Radmacher, R. W. Tillmann, M. Fritz, H. E. Gaub, *Science* **1992**, *257*, 1900. (b) M. Salmeron, G. Neubauer, A. Folch, M. Tomitori, D. F. Ogletree, P. Sautet, *Langmuir* **1993**, *9*, 3600. (c) B. Bhushan, V. N. Koinkar, *Appl. Phys. Lett.* **1994**, *64*, 1653. (d) J. P. Aime, C. Elkaakour, C. Odin, T. Bouhacina, D. Michel, J. Curely, J. Dautant, *J. Appl. Phys.* **1994**, *76*, 754.
[7] (a) A. L. Weisenhorn, P. Maivald, H.-J. Butt, P. K. Hansma, *Phys. Rev. B* **1992**, *45*, 11226. (b) N. A. Burnham, D. D. Dominguez, R. L. Mowery, R. J. Colton, *Phys. Rev. Lett.* **1990**, *64*, 1931. (c) K. O. van der Werf, C. A. J. Putman, B. G. de Grooth, J. Greve, *Appl. Phys. Lett.* **1994**, *65*, 1195. (d) D. R. Baselt, J. D. Baldeschwieler, *J. Appl. Phys.* **1994**, *76*, 33. (e) C. D. Frisbie, L. F. Rozsnyai, A. Noy, M. S. Wrighton, C. M. Lieber, *Science* **1994**, *265*, 2071.
[8] J. Tersoff, D.R. Hamman, *Phys. Rev. B* **1985**, *31*, 805.
[9] For a review, see: S. N. Magonov, M.-H. Whangbo, *Adv. Mater.* **1994**, *6*, 355.
[10] M.-H. Whangbo, R. Hoffmann, *J. Am. Chem. Soc.* **1978**, *100*, 6093.

[11] R. M. Trompt, *J. Phys. Condens. Matt.* **1989**, *1*, 10211.
[12] I. Tuzov, K. Crämer, B. Pfannemüller, S. N. Magonov and M.-H. Whangbo, *New J. Chem.*, in press.
[13] (a) Q. Zhong, D. Innis, K. Kjoller, V. B. Elings, *Surf. Sci. Lett.* **1993**, *290*, L688. (b) M. Dreier, D. Anselmetti, H.-J. Güntherodt, *J. Appl. Phys.* **1994**, *76*, 5095.
[14] (a) A. Wawkuschewski, H.-J. Cantow, S. N. Magonov, *Adv. Mater.* **1994**, *6*, 476. (b) A. Wawkuschewski, K. Crämer, H.-J. Cantow, S. N. Magonov, *Ultramicroscopy* **1995**, *58*, 185.
[15] (a) T. P. Weihs, Z. Nawaz, S. P. Jarvis, J. B. Pethica, *Appl. Phys. Lett.* **1991**, *59*, 3536. (b) J. B. Pethica, W. C. Oliver, *Phys. Scr.* 1987, *T19*, 61.
[16] (a) C. M. Mate, R. Erlandsson, G. M. McClelland, S. Chiang, *Surf. Sci.* **1989**, *208*, 473. (b) M. Salmeron, D. F. Ogletree, C. Ocal, H.-C. Wang, G. Neubauer, W. Kolbe, G. Meyers, *J. Vac. Sci. Technol. B* **1991**, *9*, 1347.
[17] D. J. Müller, G. Bült, A. Engel, *J. Mol. Biol.* **1995**, *249*, 239.
[18] (a) M.-H. Whangbo, W. Liang, J. Ren, S. N. Magonov, A. Wawkuschewski, *J. Phys. Chem.* **1994**, *98*, 7602. (b) H. Bengel, H.-J. Cantow, S. N. Magonov, L. Monconduit, M. Evain, M.-H. Whangbo, *Surf. Sci. Lett.* **1994**, *321*, L170. (c) H. Bengel, H,-J. Cantow, S. N. Magonov, H. Hillebrecht, G. Thiele, W. Liang, M.-H. Whangbo, *Surf. Sci.*, in press. (d) H. Bengel, H.-J. Cantow, S. N. Magonov, L. Monconduit, M. Evain, W. Liang, M.-H. Whangbo, *Adv. Mater.* **1994**, *6*, 649.
[19] (a) V. Y. Yaminsky, B. W. Ninham, *Langmuir* **1993**, *9*, 3618. (b) W. A. Ducker, D. R. Clarke, *Colloid. Surf.* **1994**, *94*, 275.

2 Physical Phenomena Relevant to STM and AFM

The range of applications of the scanning probe technique is determined by the nature of the probing interaction. The electron tunneling and force interactions between macroscopic bodies, which are relevant for STM and AFM, have been the subject of numerous studies in the past [1, 2]. Theoretical and experimental aspects of the physical phenomena involved in STM and AFM are discussed in this chapter.

2.1 Electron Transport Processes

One of the important factors controlling the nature of the electron transfer between the tip and the sample (i.e., at the electrodes) is the tip-sample separation. In the conventional view of STM, it is assumed that the tip-sample separation is large (Fig. 2.1 (a)) [3], although this is not necessarily true in practical applications. Therefore, it is important to consider electron transfer processes at small tip-sample separations. The theoretical studies of Ciraci [4] show that as the tip-sample separation decreases, the electron transfer process changes from the conventional tunneling regime to the electronic contact regime and to the mechanical contact regime. This analysis provides a starting point for the interplay between theory and experiment aimed at better understanding the STM and AFM operations and the associated tip-sample interactions.

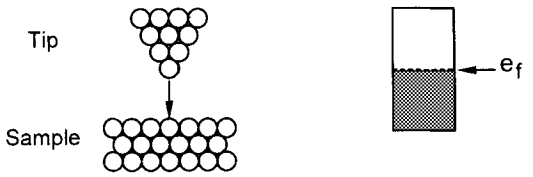

Figure 2.1 (a) Ideal tip-sample arrangement in STM. (b) Partially filled band of a metallic sample, where the Fermi level is indicated by e_f.

2.1.1 Conventional Electron Tunneling Regime

The electron transfer process in metallic tip-insulator-metal systems is classified into three mechanisms on the basis of the current-vs.-voltage (I-V) relationship [5, 6]. In tunnel emission, when the applied voltage (V) is much less than the effective barrier height (ϕ) of the insulator ($V \ll \phi/e$), the current is proportional to the applied voltage ($I \propto V$). In field emission, with $V \gg \phi/e$, the I-V dependence is given by

$$I \propto V^2 \exp(-\text{const}/V)$$

In Schottky emission, where the potential barrier is low and $V \gg k_B T/e$, the current is proportional to $\exp(\text{const}/V^{1/2})$. In the topografiner (the predecessor of the scanning tunneling microscope), which employs the field emission phenomenon, the tip-sample separation is around 100 nm. In the electron tunneling process which occurs between electrodes separated by 0.5-1 nm, the I-V dependence is linear [5].

In the tunneling regime, the tip and sample can be regarded as independent and the electron transfer between them is described by the perturbation approach, using the wave functions of the free electrodes. Representing the tip by an atom with a single s-orbital and assuming a small bias voltage between the tip and sample, Tersoff and Hamman [7] showed on the basis of the perturbation approach that the spatial variation of the tunneling current I_{tun} is described by that of the partial electron density distribution $\rho(r, e_f)$ of the sample as $I_{tun} \propto \rho(r, e_f)$. The partial electron density is associated with the energy levels lying in the vicinity of the Fermi level e_f (Fig. 2.1 (b)). The evaluation of this density distribution at the tip-sample distance of r_0 (from the sample surface) gives rise to the partial density plot $\rho(r_0, e_f)$, which simulates the observed STM image.

2.1.2 Electronic and Mechanical Contact Regimes

When the tip-sample separation is decreased below a certain distance, the overlap of their wave functions increases and the potential barrier between the electrodes is gradually lowered. This causes rearrangement of the electron density distribution and induces short-range attractive forces (adhesion) and displacements of the atoms in the tip and in the sample [4]. The local electronic and structural modifications are significant but they are reversible. Furthermore, the transport of current takes place via tunneling although the electronic states are substantially modified.

As the tip-sample distance decreases, direct tip-sample contact begins with a quantum dot contact, for which the diameter of the contact area is smaller than the mean free path of an electron. In this regime, electron transport occurs in the absence of any barrier (i.e., ballistic conduction). On further shortening of the tip-sample

distance, the gap resistance R_{gap} (i.e., the resistance between the tip and the sample) reaches the limiting value of the Sharvin resistance (i.e., $4\pi^2 e/h^2 = 13$ KΩ). Below this R_{gap} value, ohmic conductance is observed (i.e., the $I-V$ curve is linear). The current-vs.-distance dependence in the ballistic regime is rather sharp [8], so that high-resolution imaging can be achieved in this regime [9]. However, in the ballistic and ohmic contact regimes, the tip and sample may undergo an irreversible deformation due to strong force interactions (see Section 2.2).

2.1.3 STM in Different Environments

The scanning tunneling microscope was initially designed for operation in ultrahigh vacuum (UHV). It soon became clear that this instrument can be used in ambient conditions, under liquid, and in an electrochemical environment, to obtain surface images with atomic resolution. Quite strikingly, it was found that organic molecules, which are insulating, can be imaged by STM when they are adsorbed on conducting substrates [10]. So far the electron transfer mechanisms responsible for atomic-scale imaging are not well understood. One cannot exclude the possibility that the actual electron transfer mechanism can be different from conventional tunneling. The $I-V$ dependence found for ambient-condition STM measurements is consistent with Schottky emission [6], which suggests that electron transfer is facilitated by much lower barrier heights in air than in vacuum. This is believed to result from the contamination layer present between the tip and the surface. Even in UHV, surfaces can be contaminated by oxides, hydroxides, and water, thereby affecting the relationship between the current and tip-sample separation [11, 12]. It has been suggested that the low barrier heights and atomic-resolution imaging originate from intermediate-state tunneling (i.e., via the localized states of the adsorbates in the tip-sample gap) [12]. Electron transfer through the water overlayer may become a dominant process in low-current (picoamp-range) STM imaging of DNA macromolecules on mica, which was performed in humid air [13]. These observations clearly demonstrate a need for systematic experimental and theoretical studies of STM in different environments.

2.2 Survey of Force Interactions

A thorough consideration of tip-sample interactions is essential in STM and AFM, because the tip is placed very close to the sample surface. In contact-mode AFM, the atomic-scale image contrast originates from the variation of the tip-sample repulsive force and therefore contains local information due to the short-range character of this force. It is not clear whether long-range attractive forces can be used to

image surfaces with atomic resolution. Nevertheless, the attractive forces are important in AFM and STM because they contribute to the overall tip–sample interactions and hence to the size of the tip–sample contact area. The forces that the tip exerts on the sample can induce a surface deformation and add complexity to the resulting image [14].

2.2.1 Force-vs.-Distance Curves

Force-vs.-distance curves describing the interactions between two macroscopic bodies are traditionally measured with surface force apparatus [15]. The corresponding curves for the tip/sample system can be obtained with an atomic force microscope [16]. When the tip comes close to the sample, the cantilever is deflected from its equilibrium position in response to the force experienced by the tip (Fig. 2.2). It bends towards the sample when the force is attractive, and away from it when the force is repulsive. As the sample approaches the tip in the nontouching regime, the van der Waals (VDW) attraction bends the cantilever towards the sample. When the sample is moved further, at a certain point (the jump-in contact point) the attraction force gradient exceeds the spring constant of the cantilever, and the tip jumps onto the sample surface, thereby making a contact with the sample. As the sample moves further towards the tip, the cantilever is deflected as the sample is moved (the touching regime). In addition to the bending of the cantilever, the tip and sample may undergo elastic (reversible) or plastic (irreversible) deformations.

When the sample is retracted from the tip in the touching regime, the cantilever moves again with the sample. It may even deflect towards the sample before the tip breaks the contact with the sample due to the adhesive and capillary forces. The latter arise from the contamination liquid layer covering the sample surface in air. The tip loses contact with the sample surface at the jump-out point, where the transition from touching to nontouching occurs, and the force-vs.-distance curve returns to the

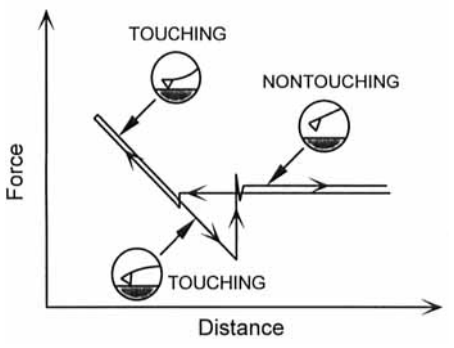

Figure 2.2 Typical force-vs.-distance curve observed in AFM experiments in air.

nontouching line. The difference between the minimum point of the "retrieval" force-vs.-distance curve and the nontouching line is defined as the pull-out force, which becomes identical to the adhesive force when the capillary force vanishes.

In the attractive force region where the force-vs.-distance curve exhibits hysteresis, the behavior of the probe is strongly influenced by the long-range forces. Details of the curve can vary significantly, depending on the nature of the tip and sample (e.g., metallic or insulating) as well as on the medium in which they are immersed. For example, when the nonconducting tip and sample are immersed in water, the pull-out forces are reduced to the level of 1 nN or less [16]. In the repulsive force region, the mechanical response of the sample depends on the hardness of the sample, that of the tip, and the force constant of the cantilever.

2.2.2 Short-Range Forces and Sample Deformation

Short-range force interactions between atoms are often described on the basis of atom-atom pair potentials such as Lennard-Jones or Morse type potentials [2a]. They are strongly repulsive at a short distance and slightly attractive at a long distance, so the short-range repulsive interaction is more sensitive to a small change in the distance than is the long-range attractive interaction. This leads to a sharp force-vs.-distance relationship and provides the basis for a high-resolution surface imaging in contact-mode AFM.

An important question concerning contact AFM is: which property of the sample controls the tip-sample repulsive force? At the computational level, Gordon and Kim provided an efficient and reliable method to calculate the forces between closed-shell atoms and molecules in the regions of the attractive well and the repulsive wall [17]. In this method, the interaction energies are calculated on the basis of the electron densities of the interacting systems. To a first approximation, therefore, the spatial variation of the tip-sample repulsive force F_{rep} should be described by that of the total electron density $\rho(r)$ of the sample, as $F_{rep} \propto \rho(r)$. The evaluation of this density distribution at the tip-sample distance of r_0 (from the sample surface) gives rise to the total density plot $\rho(r_0)$, which simulates the observed AFM image.

In many contact-mode AFM experiments and in ambient-condition STM measurements, the tip-sample repulsive interactions are strong enough to induce a surface deformation during the scanning. The simple case of an elastic contact between a sphere pressed into a flat surface (Fig. 2.3) was analyzed by Hertz [18], who correlated the contact characteristics (e.g., the load, contact area, and indentation depth) with the mechanical properties of two interacting bodies (e.g., Young's moduli and Poisson's ratios). Hertz theory, commonly used in the analysis of macroscopic hardness tests, was also applied by Pethica and co-workers [19] to describe the tip-sample interactions in STM and AFM. This study allows one to estimate the size of the tip-sample contact area (e.g., for a tungsten tip of 20 nm radius acting on an or-

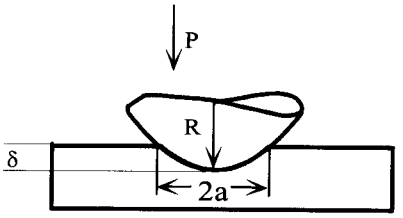

Figure 2.3 Deformation of the sample surface produced by the tip with apex radius r, where a is the radius of the contact area and δ is the surface depression.

ganic sample under an applied force of 1 nN, the diameter of the contact area is about 2.3 nm). It should be recalled that Hertz theory is valid only for an elastic deformation in a nonadhesive contact. In reality, contacting bodies deform according to their elastic as well as inelastic properties, and the surface forces bring about adhesion [20], thereby leading to a contact area greater than that given by Hertz theory. Several theories concerning the deformations and adhesion of contacting bodies predict [21, 22] a nonzero contact area even at zero applied force. In general, it is difficult to describe solids in contact even for bodies of ideal geometrical shape, because the stress distribution in the solids depends on the surface interaction, which in turn depends on the exact shape of the deformed surfaces [20]. All these continuum theories deal with the experimental results obtained by the surface force apparatus and the hardness tester (nanoindenter) [23].

Macroscopic contacts between bodies are involved in the operation of both STM and AFM instruments, and the diameter of the tip–sample contact area is on the order of several nanometers. In addition, both scanning tunneling and atomic force microscopes provide atomic-scale images of the surfaces deformed by the tip force during the scanning. Therefore, invaluable information about the nanomechanical surface properties can be obtained by these methods. How the sample surface is deformed under the tip force (when the tip is harder than the sample) can be tentatively envisioned as follows. The region of the sample in contact with the tip undergoes a macroscopic deformation as predicted by the continuum theories in which the sample is regarded as a body of homogeneous density distribution. In most cases of chemical interest, the surface of a sample consists of atoms with several different environments, so that the local hardness of the surface varies from place to place. Therefore, the strong tip force induces a surface deformation according to the local hardness variation [14, 24, 25]. Such a deformation, which can be on the nanometer or even atomic scale, is superposed on the macroscopic one (Fig. 2.4). The experimental evidence for this phenomenon is presented in Chapter 9.

During scanning in contact-mode AFM, the tip moves laterally so that the cantilever experiences vertical (normal) as well as lateral (friction) forces. Therefore, measurements of the lateral force variation in AFM experiments allow one to examine the

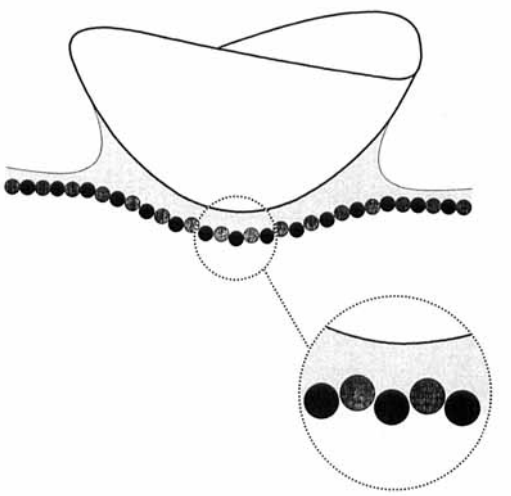

Figure 2.4 Superposition of the macroscopic and microscopic deformations of the sample surface under the tip force.

tip–surface friction from the micron scale down to the atomic scale. Currently, it is the subject of intensive studies to test the feasibility of using AFM for the analysis of friction. The recent study of Salmeron and co-workers [26] with a silicon nitride (Si_3N_4) tip on mica showed that the frictional forces are proportional to the normal forces (i.e., loads) in the moderate range (10–80 nN), in agreement with the friction behavior of macroscopic systems [27]. (At low loads a nonlinear behavior of the friction versus load is observed, due to the surface forces and the presence of the weakly adsorbed layers on the surface.) There have been numerous observations of atomic-scale friction behavior (e.g., the dependence of the friction force on the load as well as the scanning speed and direction) [28]. To analyze such experimental data, one should consider the atomic-scale surface corrugations and the possible tip-force induced surface relaxation. The importance of the surface corrugations to the friction behavior has been demonstrated theoretically and experimentally [29–31]. The tip-force induced surface relaxation was estimated to be small (below 0.1 nm) for the combination of a diamond-tip with a diamond surface [28], but the same cannot be expected for other systems. In analyzing the frictional data from AFM experiments, one should consider the tip-force induced corrugations – the macroscopic ones described by the continuum theories as well as the microscopic ones expected from the variation of the surface local hardness.

2.2.3 Long-Range and Other Forces

2.2.3.1 Long-Range Forces

Bodies at separations well beyond the chemical bonding distances experience VDW interactions, which can occur even when the electronic states of the separated bodies are decoupled. The VDW forces are important in STM and AFM because, depending on the shape of the tip, the atoms at the tip apex experience strong repulsion and deformation due to the VDW attraction between the sample and the back of the tip apex [32–34]. The magnitude of the VDW forces for the model tip/sample systems relevant to STM and AFM is estimated to be in the 1–20 nN range [32].

According to Lifshitz theory [35], the VDW forces are considered as dispersion forces associated with the electromagnetic fluctuations. This theory shows that the forces between bodies interacting through a medium depend on the dielectric properties of the bodies and the medium, and they are generally attractive but can also be repulsive. (The latter happens for the interaction of different bodies immersed in a medium, when the refractive index and dielectric constant of the medium have values lying between the corresponding values of the bodies.) Measurements of the forces between macroscopic bodies separated in the 50–250 nm range show that Lifshitz theory is in good agreement with experiment [2b].

It should be noted that not all long-range interactions follow the predictions of Lifshitz theory. For example, the attractive VDW forces between hydrophobic solids immersed in aqueous media exceed the expected theoretical values by one or two orders of magnitude [36]. This hydrophobic attraction was explained by Yaminsky and Ninham [37], who showed that fluctuations in molecular density give rise to long-range effects similar to the electromagnetic effects associated with charge density fluctuations. Their analysis of the molecular fluctuation shows that the approach of two surfaces in a poorly wetting liquid decreases the density of the liquid in the gap, due to enhancement of the thermal fluctuations in the lateral direction (Fig. 2.5 (a)). This lateral decompression manifests itself as the attractive force acting between two surfaces. For the case of two hydrophilic solids immersed in a medium (Fig. 2.5 (b)), the density of the liquid in the gap increases if the components of the medium possess higher affinity for the solid than for each other. The compression effect manifests itself as the repulsive forces acting between the two solid surfaces. This hydro-

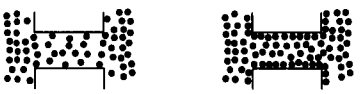

Figure 2.5 (a) Density decrease in the gap between two hydrophobic bodies immersed in an aqueous medium. (b) Density increase in the gap between two hydrophilic bodies immersed in an aqueous medium. (Adapted from Ref. 37)